
C-LoRA: Contextual Low-Rank Adaptation for Uncertainty Estimation in Large Language Models

Amir Hossein Rahmati¹ Sanket Jantre² Weifeng Zhang¹ Yucheng Wang¹
 Byung-Jun Yoon^{1,2} Nathan M. Urban² Xiaoning Qian^{1,2}

¹Texas A&M University, College Station, TX ²Brookhaven National Laboratory, Upton, NY
 {amir_hossein_rahmati, weifengzhang, wangyucheng, bjyoon, xqian}@tamu.edu
 {sjantre, nurban, byoon, xqian1}@bnl.gov

Abstract

Low-Rank Adaptation (LoRA) offers a cost-effective solution for fine-tuning large language models (LLMs), but it often produces overconfident predictions in data-scarce few-shot settings. To address this issue, several classical statistical learning approaches have been repurposed for scalable uncertainty-aware LoRA fine-tuning. However, these approaches neglect how input characteristics affect the predictive uncertainty estimates. To address this limitation, we propose Contextual Low-Rank Adaptation (**C-LoRA**) as a novel uncertainty-aware and parameter efficient fine-tuning approach, by developing new lightweight LoRA modules contextualized to each input data sample to dynamically adapt uncertainty estimates. Incorporating data-driven contexts into the parameter posteriors, C-LoRA mitigates overfitting, achieves well-calibrated uncertainties, and yields robust predictions. Extensive experiments demonstrate that C-LoRA consistently outperforms the state-of-the-art uncertainty-aware LoRA methods in both uncertainty quantification and model generalization. Ablation studies further confirm the critical role of our contextual modules in capturing sample-specific uncertainties. C-LoRA sets a new standard for robust, uncertainty-aware LLM fine-tuning in few-shot regimes.

1 Introduction

Large Language Models (LLMs) [1–7] have shown their promising potential in diverse areas [8–18]. Due to their general-purpose language understanding and generation capabilities with human-level performance [1, 2], fine-tuning LLMs to various downstream tasks has drawn significant attention [19–23]. However, when fine-tuned for downstream tasks with limited data, LLMs may hallucinate to produce overconfident results, which becomes a serious concern [24–27]. To address this, reliable estimation of uncertainty has become essential [19, 20, 28].

To enable predictive uncertainty quantification (UQ), probabilistic inference with Bayesian neural network (BNN) has been studied in deep learning [29–41], where neural network weights are treated as random variables with variational inference (VI) approximating the true posterior to provide reliable UQ [42, 43]. Adopting these approaches for LLMs is limited by their prohibitive computational and memory costs compared to conventional methods [19, 20, 22], making full Bayesian fine-tuning of all the parameters of an LLM challenging.

Parameter Efficient Fine-Tuning (PEFT) methods, such as Low-rank Adaptation (LoRA), substantially reduce the number of learnable parameters and thereby mitigate the significant computational expenses and excessive memory utilization [21, 44–48]. This efficiency facilitates employing Bayesian methods for UQ in LLMs [19, 20, 49–51]. Most of the recent studies considered a more straightforward solution, like in [49–51] where authors considered ensemble methods. [19] proposed a *post-hoc*

Bayesian inference method for the LoRA adapters using Laplace approximation [34]. [20] repurposed a mean-field VI based Bayesian framework for LoRA-based fine-tuning to jointly estimate the LoRA parameters’ variational means and variances [20]. However, the uncertainty stemming from data, *aleatoric uncertainty*, has not been considered in the existing methods, leading to poor performance especially when fine-tuning with limited data. This motivates us to focus on incorporating aleatoric uncertainty for a novel parameter efficient fine-tuning approach in this work.

We propose **Contextual Low-Rank Adaptation, C-LoRA**, which enables an explicit consideration of aleatoric uncertainty (data uncertainty). This formulation not only leads to faster training, but also provides a sample-dependent uncertainty estimation for each layer, which leads to beneficial and more favorable uncertainty-aware LLM fine-tuning under small-data scenarios. In particular, we introduce a contextual module for modeling the stochasticity in low-dimensional space dependent on the data, which enables a low-cost contextualized estimation of prediction uncertainty in terms of computation and memory usage. Our contributions can be outlined as follows:

- We propose a new end-to-end Bayesian framework for scalable uncertainty-aware LLM fine-tuning via contextualized LoRA on data in the lower-dimensional space by a flexible contextual module;
- Our framework allows for efficient modeling of aleatoric (data) uncertainty;
- We showcase the superiority of C-LoRA regarding both UQ capabilities and generalizability via extensive experiments across different tasks;
- Through ablation experiments, we demonstrate the significance of our new contextual module on achieving better UQ while offering consistent prediction accuracy.

2 Preliminaries

In this paper, vectors and matrices are denoted by bold lowercase and uppercase letters, respectively. Most of our mathematical notations follow the ones adopted in [21], [19], [20], and [39].

2.1 Low-Rank Adaptation (LoRA)

LoRA, a parameter-efficient fine-tuning approach, adapts a pre-trained language model to downstream tasks [21]. It rests on the assumption that the required weight updates have a low intrinsic dimensionality, so LoRA freezes the original weights and instead learns low-rank update matrices. To this end, the modified forward pass becomes:

$$\mathbf{h} = (\mathbf{W}_0 + \Delta\mathbf{W})\mathbf{x} = (\mathbf{W}_0 + \mathbf{B}\mathbf{A})\mathbf{x}, \quad (1)$$

where $\mathbf{x} \in \mathbb{R}^k$ and $\mathbf{h} \in \mathbb{R}^d$ are input and output vectors, respectively, and $\mathbf{W}_0 \in \mathbb{R}^{d \times k}$ represents the frozen pre-trained weights. LoRA inserts two low-rank update factors $\mathbf{B} \in \mathbb{R}^{d \times r}$ and $\mathbf{A} \in \mathbb{R}^{r \times k}$ with $r \ll \min(d, k)$. Hence, the number of trainable parameters reduces to $r \times (d + k)$ which is considerably lower than $d \times k$ in the full matrix. This dramatically cuts storage and computational costs while matching full-matrix fine-tuning performance. Here on, we set $k = d$, so that $\mathbf{W}_0 \in \mathbb{R}^{d \times d}$.

2.2 Bayesian Uncertainty Estimation

Let $\mathcal{D} = \{\mathbf{x}_i, y_i\}_{i=1}^N$ be a dataset of N independent and identically distributed (i.i.d.) observations, where each \mathbf{x}_i is an input sample and y_i is the corresponding output. In the Bayesian paradigm, rather than selecting a single best-fit model parameterization, we maintain a distribution over all plausible model parameters. Specifically, given model parameters θ , Bayesian inference aims to characterize the posterior distribution $p(\theta|\mathcal{D})$ using Bayes’ rule: $p(\theta|\mathcal{D}) \propto p(\mathcal{D}|\theta)p(\theta)$, where $p(\mathcal{D}|\theta)$ is the likelihood of the observed data under parameters θ , and $p(\theta)$ is the prior distribution reflecting beliefs about θ before seeing any data.

To generate predictions for a new input \mathbf{x}^* , Bayesian model averaging, which integrates over the posterior is applied and the intractable integral is approximated using Monte Carlo sampling:

$$p(y^*|\mathbf{x}^*, \mathcal{D}) = \int p(y^*|\mathbf{x}^*, \theta)p(\theta|\mathcal{D})d\theta \approx \frac{1}{M} \sum_{m=1}^M p(y^*|\mathbf{x}^*, \theta_m), \quad \theta_m \sim p(\theta|\mathcal{D}). \quad (2)$$

2.3 Bayesian Low-Rank Adaptation

Despite the existence of scalable posterior inference methods, a full Bayesian treatment of LLMs remains computationally prohibitive. By restricting Bayesian updates to the LoRA parameters, a

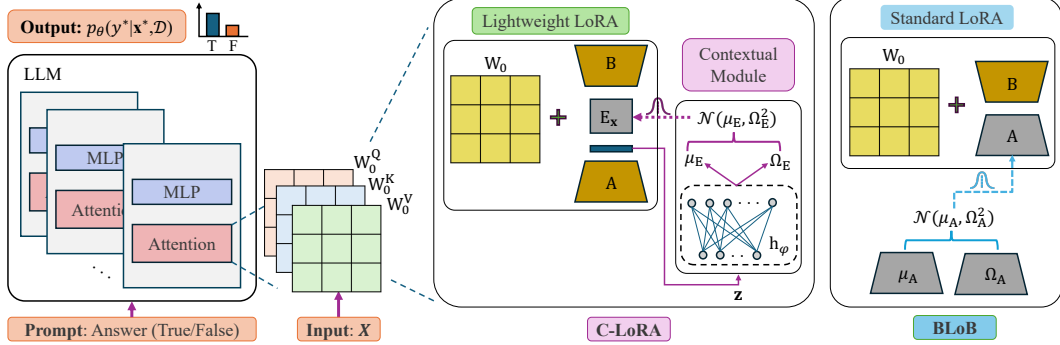


Figure 1: A visual representation of our proposed method, Contextual LoRA (**C-LoRA**) and the Bayesian LoRA by backpropagation (**BLoB**).

tractable uncertainty quantification scheme can be achieved; however, even Markov chain Monte Carlo (MCMC) over millions of LoRA weights is too costly. As a practical compromise, *Bayesian LoRA by backpropagation (BLoB)* [20] embeds uncertainty estimation directly into fine-tuning via mean-field variational inference on LoRA adapters. More specifically, they keep \mathbf{B} deterministic in (1) and Bayesianize \mathbf{A} with a variational distribution $q(\mathbf{A}) = \mathcal{N}(\mathbf{A} | \mu_{\mathbf{A}}, \Omega_{\mathbf{A}}^2)$, where $\mu_{\mathbf{A}}$ and $\Omega_{\mathbf{A}}^2$ are the variational mean and variance estimates, respectively. To this end, they learn the variational distribution parameters by maximizing the Evidence Lower Bound (ELBO):

$$\mathcal{L}' = \mathbb{E}_q [\log p(\mathcal{D} | \mathbf{A}, \mathbf{B})] - \text{KL}[q(\mathbf{A}) \| p(\mathbf{A})]. \quad (3)$$

Here, the first term measures the expected negative log-likelihood of the data under the variational posterior, while the second term is the Kullback-Leibler (KL) divergence between the variational posterior and the prior, acting as a regularization. Using the reparameterization trick, BLoB jointly updates means and variances providing scalable, predictive uncertainty estimates. A visual representation of BLoB framework is presented in Figure 1.

3 Contextual Low-Rank Adaptation (C-LoRA)

We introduce the formulation of Contextual Low-Rank Adaptation (C-LoRA), which enables scalable, efficient, data-dependent uncertainty quantification at the sample level. First, we introduce a lightweight LoRA factorization to reduce the computational burden of variational inference in Bayesian LoRA. Based on this factorization, we treat the LoRA weights' stochasticity to be data-dependent, and learn the weight distribution parameters via a variational Bayesian objective.

3.1 Lightweight LoRA Factorization

The standard LoRA update in (1) introduces two low-rank matrices whose size scales with the frozen weight dimension d , so that any Bayesian treatment—whether both adapters are stochastic or only \mathbf{A} is (as in BLoB)—incurs a computational cost that grows linearly in d . To break this dependency, we insert a low-dimensional matrix $\mathbf{E} \in \mathbb{R}^{r \times r}$ between \mathbf{B} and \mathbf{A} . This modification reduces the stochastic parameter complexity to a constant in d , yielding a modified LoRA factorization as follows

$$\mathbf{h} = (\mathbf{W}_0 + \Delta \mathbf{W})\mathbf{x} = (\mathbf{W}_0 + \mathbf{B}\mathbf{E}\mathbf{A})\mathbf{x}. \quad (4)$$

Compared to the BLoB mean-field VI framework, this new factorization facilitates a more scalable, lightweight Bayesian LoRA by inferring a distribution over the elements of \mathbf{E} elements while learning \mathbf{B} and \mathbf{A} deterministically, making data-dependent Bayesianization of LoRA fine-tuning scalable.

3.2 Contextualized Parameter Uncertainty

In conventional Bayesian neural networks, the focus is on epistemic uncertainties introduced by treating model parameters as random variables drawn from a fixed distribution—one that does not depend on the input data. This leads to model parameters that can vary from data to data, while their distribution remains invariant for all the samples within given training data. This severely limits the uncertainty estimates in few-shot LoRA fine-tuning settings. To address this, we propose

a data-dependent, or *contextual*, Bayesian fine-tuning paradigm, wherein the distribution of the parameters of low-rank adapters depends on the inputs \mathbf{x}_i for each data sample (\mathbf{x}_i, y_i) . Although one could perform Bayesian inference over \mathbf{B} and \mathbf{A} LoRA adapters from (1), this scales linearly with the frozen weight dimension d . Instead, by leveraging the lightweight LoRA factorization from (4), we learn the low-dimensional \mathbf{E} matrix contextually, yielding the weight updates as

$$\Delta \mathbf{W} = \mathbf{B} \mathbf{E}_x \mathbf{A} \quad (5)$$

where \mathbf{E}_x denotes the data-dependent version of \mathbf{E} . Next, we infer \mathbf{E}_x by defining a variational distribution $q_\phi(\mathbf{E}_{\mathbf{x}_i} | \mathbf{x}_i) = \mathcal{N}(\boldsymbol{\mu}_{\mathbf{E}}(\mathbf{x}_i), \boldsymbol{\Omega}_{\mathbf{E}}^2(\mathbf{x}_i))$. We learn these distribution parameters by introducing a lightweight auxiliary contextual module comprising of a small neural network with parameters φ . From the perspective of amortized variational inference, q_ϕ can be viewed as inference network (encoder) approximating the posterior $p(\mathbf{E}_{\mathbf{x}_i} | y_i, \mathbf{x}_i) \propto p(y_i | \mathbf{x}_i, \mathbf{E}_{\mathbf{x}_i}) p(\mathbf{E}_{\mathbf{x}_i})$. The inference network parameters ϕ only depend on \mathbf{x}_i since y_i is unavailable during testing. To infer the model posterior, we optimize the corresponding ELBO of the evidence $\sum_i \log p(y_i | \mathbf{x}_i) = \sum_i \log \int p(y_i | \mathbf{x}_i, \mathbf{E}_{\mathbf{x}_i}) p(\mathbf{E}_{\mathbf{x}_i}) d\mathbf{E}_{\mathbf{x}_i}$ given $q_\phi(\mathbf{E}_{\mathbf{x}_i} | \mathbf{x}_i)$:

$$\mathcal{L} = \sum_{i=1}^N \left[\mathbb{E}_{q_\phi(\mathbf{E}_{\mathbf{x}_i} | \mathbf{x}_i)} \log p_\theta(y_i | \mathbf{x}_i, \mathbf{E}_{\mathbf{x}_i}) - \text{KL}(q_\phi(\mathbf{E}_{\mathbf{x}_i} | \mathbf{x}_i) \| p(\mathbf{E}_{\mathbf{x}_i})) \right]. \quad (6)$$

Here, θ represents \mathbf{B} and \mathbf{A} collectively. Unlike standard variational inference as in (3), our formulation makes the distribution of $\mathbf{E}_{\mathbf{x}_i}$ input-dependent and replaces the single KL term with a sum of N per-sample KL divergences, whose combined impact scales with N . More importantly, we focus exclusively on *aleatoric uncertainty*—modeling the variability in y_i given \mathbf{x}_i —with the epistemic uncertainty modeling available via imposing prior on φ or Bayesianizing \mathbf{A} or \mathbf{B} when needed, thereby isolating and highlighting the advantages of data-dependent aleatoric UQ.

Sequential Cross-Layer Dependency. Consider a pre-trained LLM with L layers, each augmented by its own LoRA adapters $\mathbf{B}^l, \mathbf{E}_{\mathbf{x}}^l$, and \mathbf{A}^l . We model $\mathbf{E}_{\mathbf{x}_i}^l$ in an autoregressive manner, so that its distribution depends on $\{\mathbf{E}_{\mathbf{x}_i}^j\}_{j < l}$, leading to $q_\phi(\mathbf{E}_{\mathbf{x}_i}^l | \mathbf{x}_i) = \prod_{l=1}^L q_\phi(\mathbf{E}_{\mathbf{x}_i}^l | \mathbf{x}_i^{l-1})$, where \mathbf{x}_i^{l-1} denotes the output of layer $l-1$ and is a function of $\{\mathbf{E}_{\mathbf{x}_i}^1, \dots, \mathbf{E}_{\mathbf{x}_i}^{l-1}, \mathbf{x}_i\}$.

3.3 Auxiliary Contextual Module Parameterization

In layer l , given $\mathbf{z}^l = \mathbf{A}^l \mathbf{x}^{l-1} \in \mathbb{R}^r$ as input, the contextual module denoted by h_φ^l produces the parameters $(\boldsymbol{\mu}_{\mathbf{E}}^l, \boldsymbol{\Omega}_{\mathbf{E}}^l)$ of the $\mathbf{E}_{\mathbf{x}}^l$ distribution as output. We then draw $\mathbf{E}_{\mathbf{x}}^l$ conditioned on $\boldsymbol{\mu}_{\mathbf{E}}^l$ and $\boldsymbol{\Omega}_{\mathbf{E}}^l$. Then, multiplying $\mathbf{B}^l, \mathbf{E}_{\mathbf{x}}^l$, and \mathbf{z}^l and adding it to $\mathbf{W}_0^l \mathbf{x}^{l-1}$ yields the output of the layer l , \mathbf{x}^l . We parameterize the per-layer contextual module with a neural network with two fully-connected layers, parametrized by φ . In particular, the neural network has r inputs, C hidden units, and $2 \times r^2$ outputs with the nonlinear ReLU activation function connecting the two fully-connected layers.

3.4 Variational Bayesian Objective

Our optimization objective for C-LoRA fine-tuning is as given in (6). We adopt a simple and fixed Gaussian prior $p(\mathbf{E}_{\mathbf{x}})$ for learning $\mathbf{E}_{\mathbf{x}}$ in each layer. The complete learning objective can be expressed as a summation over all samples: $\mathcal{L} = \sum_{(\mathbf{x}, y) \in \mathcal{D}} \mathcal{L}(\mathbf{x}, y)$. Then, we learn the deterministic parameters \mathbf{B} and \mathbf{A} together represented by θ using the expected negative log-likelihood (NLL) term while excluding the KL term. This ensures that learning θ remains supervised, yielding less noisy gradients per sample computed as

$$\nabla_\theta \mathcal{L}(\mathbf{x}, y) = \mathbb{E}_{q_\phi(\mathbf{E}_{\mathbf{x}} | \mathbf{x})} \nabla_\theta \log p_\theta(y | \mathbf{x}, \mathbf{E}_{\mathbf{x}}). \quad (7)$$

We approximate this expectation with a single Monte Carlo draw $\mathbf{E}_{\mathbf{x}} \sim q_\phi(\mathbf{E}_{\mathbf{x}} | \mathbf{x})$ for each \mathbf{x} sample.

Next, to update the auxiliary network parameters φ , which appear in both the NLL and KL terms of (6), we apply the reparameterization trick [52] to handle random sampling of $\mathbf{E}_{\mathbf{x}}$. Concretely, in each layer, $\mathbf{E}_{\mathbf{x}}^l \sim \mathcal{N}(\boldsymbol{\mu}_{\mathbf{E}}^l, \boldsymbol{\Omega}_{\mathbf{E}}^l)$ is reparameterized as $\mathbf{E}_{\mathbf{x}}^l = \boldsymbol{\mu}_{\mathbf{E}}^l + \boldsymbol{\Omega}_{\mathbf{E}}^l \odot \mathcal{E}^l$, where $\mathcal{E}^l \in \mathbb{R}^{r \times r}$ is sampled from $\mathcal{N}(\mathbf{0}, \mathbf{I})$. Similarly, sampling the sequence of $\mathbf{E}_{\mathbf{x}}^l$ for all the layers using the distribution $q_\phi(\mathbf{E}_{\mathbf{x}} | \mathbf{x})$ is rewritten as $g_\phi(\mathcal{E}, \mathbf{x})$, where g_ϕ is a deterministic and differentiable mapping. With this, the gradient of the fine-tuning objective \mathcal{L} with respect to φ can now be computed as

$$\nabla_\varphi \mathcal{L}(\mathbf{x}, y) = \mathbb{E}_{\mathcal{E} \sim \mathcal{N}(\mathbf{0}, \mathbf{I})} \left[\nabla_\varphi \left(\log p_\theta(y | \mathbf{x}, g_\phi(\mathcal{E}, \mathbf{x})) - \log \frac{q_\phi(g_\phi(\mathcal{E}, \mathbf{x}) | \mathbf{x})}{p(g_\phi(\mathcal{E}, \mathbf{x}))} \right) \right]. \quad (8)$$

3.5 Testing and Computational Complexity

Test-time Sampling. Once C-LoRA training has converged, we obtain point estimate of the fine-tuned model by replacing \mathbf{E}_x with its variational mean and computing $p(y|\mathbf{x}, \mu_{\mathbf{E}}(\mathbf{x}))$. As shown in Section 4, we denote these point estimate models by setting M in our model names. Next, to demonstrate the quality of uncertainty estimation, we sample \mathbf{E}_x from its inferred distribution M times and, similar to (2), approximate the posterior predictive distribution using Monte Carlo sampling, yielding $p(y_{\text{test}}|\mathbf{x}_{\text{test}}, \mathcal{D}) = 1/M \sum_{m=1}^M p(y|\mathbf{x}, \mathbf{E}_x^m)$, where $\mathbf{E}_x^m \sim q_{\phi}(\mathbf{E}_x|\mathbf{x})$. For example, for these calibrated models with $M = 10$ drawn samples in Section 4, we label them with “M=10” in our model names. When “M=0”, the posterior mean is used directly for evaluation.

Computational Complexity. In layer l , the contextual module is designed to model $q_{\phi}(\mathbf{E}_x^l|\mathbf{x}^{l-1})$ where \mathbf{x}^l is derived from natural language; hence, learning features from scratch becomes both non-trivial and computationally expensive. To mitigate this issue, we follow [39] and take advantage of the main model by feeding \mathbf{z}^l into the contextual module instead. Additional computational cost of $\mathcal{O}(r^4)$, stems from the auxiliary network h_{ϕ}^l , whose fully connected layers have size $C = \mathcal{O}(r^2) \ll d$. This overhead is minimal compared to the main model’s per-layer operation cost of $\mathcal{O}(d^2)$. As a result, we can efficiently estimate uncertainty at the sample level in a low-dimensional space, sidestepping the costly feature-learning burden within the contextual modules during fine-tuning.

4 Experiments

In this section, we conduct comprehensive experiments to demonstrate the effectiveness of our proposed C-LoRA approach for uncertainty quantification in LLMs on reasoning datasets from various domains. We first specify the experimental settings in Section 4.1, including baselines, fine-tuning setting, and evaluation metrics. We then benchmark C-LoRA against existing uncertainty quantification methods across six reasoning datasets to evaluate overall task performance and uncertainty quality in Section 4.2. Additionally, we test the robustness of each method under distribution shift by fine-tuning on OBQA and evaluating on related OOD datasets in Section 4.3. Lastly, we perform an ablation to demonstrate the role of our auxiliary contextual module in Section 4.4.

4.1 Experimental Settings

Baselines. We provide performance comparisons of **C-LoRA** with well-established cutting-edge baselines that include Deep Ensemble [49, 51, 53], Monte-Carlo dropout (**MCD**) [29], Bayesian LoRA with Backpropagation (**BLoB**) [20], a recent mean-field VI approach applied to LoRA parameters; Laplace-LoRA (**LA**) [19], which uses a Laplace approximation over adapter weights; and *Maximum A Posteriori* (**MAP**), representing a deterministic point-estimate baseline.

LLM fine-tuning settings. Following prior work, we evaluate the performance of **C-LoRA**¹, by fine-tuning **LLaMA2-7B**[6] using the PEFT library[54] across six commonsense reasoning benchmarks, including both binary and multiple-choice classification tasks. For each task, the appropriate next-token logits are selected based on the format of the target output, which we include in the Appendix, and the model is trained to maximize the log-likelihood of the correct answer. Following previous works [20, 21, 28], we apply LoRA to the query, value, and output projection layers using default hyperparameters. All models are fine-tuned with a batch size of 4. Baseline methods are trained for 5000 iterations, while **C-LoRA** is trained for 1500 iterations on all datasets, except for Winogrande-medium (WG-M), which is trained for 2000 iterations. To ensure consistent evaluation, we curate a training-validation split by reserving 80% of the original training set for fine-tuning and holding out the remaining 20% as a validation set. This validation split is used for early stopping and checkpointing based on a metric combining validation accuracy and calibration quality (see Appendix). **Evaluation metrics.** We report results using three key evaluation metrics: accuracy (ACC), expected calibration error (ECE), and negative log-likelihood (NLL). While ACC reflects raw predictive performance, ECE and NLL are widely adopted metrics for assessing the quality of uncertainty estimates. ECE measures the alignment between predicted confidence and actual correctness, while NLL evaluates the sharpness and correctness of the model’s predicted probability distribution. All reported results are averaged over three independent runs with different random seeds, and we report the mean \pm standard deviation for each metric.

¹Using contextual modules comprising of two fully connected layers with 64 hidden units (C=64) each.

4.2 Evaluation Results under In-distribution Fine-tuning

In this section, we conduct our assessment of fine-tuning performances under the in-distribution scenario for six common-sense reasoning tasks. These tasks encompass: Winogrande-small (WG-S), Winogrande-medium (WG-M) [55], ARC-Challenge (ARC-C), ARC-Easy (ARC-E) [56], Open-BookQA (OBQA) [57], and BoolQ [58]. For all the experiments, the same pre-trained LLaMA2-7B was used as the LLM backbone. For BLoB, we kept the same setting as in [20].

Accuracy and Uncertainty Quantification Table 1 presents the performance of various uncertainty quantification methods applied to LoRA-tuned LLaMA2-7B across six common-sense reasoning datasets. Our proposed method, C-LoRA, as well as the baseline BLoB, are evaluated under both deterministic ($M=0$) and stochastic ($M=10$) posterior sampling settings. While C-LoRA, does not achieve the highest accuracy, it maintains competitive performance across all datasets, with accuracies that are typically within 1–2% of the best methods (e.g., ARC-C: 67.79%, OBQA: 78.26%). Notably, C-LoRA ($M=0$)—which uses the posterior mean without sampling—performs similarly or slightly better than the sampled version on some tasks (e.g., ARC-C: 69.02% vs. 67.79%), suggesting that the contextual posterior mean alone offers a robust deterministic approximation.

The strength of C-LoRA becomes more apparent when examining uncertainty calibration, as measured by expected calibration error (ECE). Here, C-LoRA ($M=10$) consistently achieves the lowest or second-lowest ECE across all datasets, including WG-S (6.86%), ARC-C (8.83%), ARC-E (4.27%), WG-M (3.71%), and BoolQ (1.62%). These values are significantly better than those obtained by MAP, MCD, and even Deep Ensemble, indicating that C-LoRA produces confidence estimates that are closely aligned with actual correctness. Even the deterministic variant, C-LoRA ($M=0$), outperforms BLoB ($M=10$) in calibration on datasets such as WG-S (7.16% vs. 11.23%) and performs comparably on BoolQ (1.46% vs. 1.46%). A similar pattern holds for negative log-likelihood (NLL), which reflects the quality of probabilistic predictions. C-LoRA ($M=10$) achieves among the lowest NLL values in nearly all cases, such as 0.63 on WG-S, and 0.88 on ARC-C, often outperforming both BLoB ($M=10$) and Deep Ensemble. Additionally, C-LoRA ($M=0$) matches or slightly outperforms BLoB ($M=10$) in NLL on several tasks (e.g., ARC-C: 0.89 vs. 0.88), while avoiding the computational overhead of posterior sampling. In summary, while C-LoRA trades off a small amount of accuracy compared to non-Bayesian methods, it delivers substantial improvements in calibration and likelihood, which are essential for uncertainty-aware applications.

Post-hoc Calibration with Temperature Scaling To further evaluate calibration, we apply *post-hoc* temperature scaling [59] to both BLoB and C-LoRA and report the resulting ECE on six common-sense reasoning tasks in Table 2. Even before temperature scaling, C-LoRA ($M=10$) achieves stronger calibration than BLoB on nearly every dataset. After applying temperature scaling, C-LoRA ($M=0$, tmp) achieves the best or second-best ECE in 4 of the 6 datasets, including WG-S (4.00%), ARC-E (3.86%), ARC-C (6.30%), and WG-M (2.90%). Notably, it outperforms BLoB ($M=10$, tmp) in 5 out of the 6 datasets, despite using no posterior sampling. Interestingly, C-LoRA ($M=10$, tmp) does not always show improvement over its uncalibrated variant. On datasets like OBQA and BoolQ, temperature scaling can actually worsen ECE (e.g., from 4.00% to 6.27% on OBQA). This may be due to the fact that posterior sampling already flattens the predictive distribution, and further scaling can overcorrect, leading to underconfident predictions. These results suggest that C-LoRA ($M=0$) provides an effective balance between calibration quality and inference efficiency.

4.3 Robustness Under Distribution Shift

Table 3 presents model performance under both in-distribution (OBQA) and out-of-distribution (OOD) settings with smaller (ARC-E, ARC-C) and larger (Chem, Phy) distribution shifts. While C-LoRA does not achieve the highest accuracy under shift, it demonstrates strong robustness in uncertainty estimation, especially in calibration (ECE) and likelihood (NLL). In terms of accuracy, Deep Ensemble and BLoB generally maintain higher predictive performance across OOD datasets. However, C-LoRA ($M=10$) remains competitive, achieving 65.09% accuracy on ARC-C and 41.00% on Chem—nearly matching the highest-performing methods. While C-LoRA ($M=10$) sees a slight drop in accuracy under severe shift (e.g., Phy: 31.00%), it significantly outperforms all baselines in ECE and NLL, indicating more reliable and calibrated uncertainty estimates.

For calibration (ECE), C-LoRA ($M=10$) achieves the lowest error on Chem (12.49%) and ARC-C (8.83%). This trend also holds for Phy, where C-LoRA ($M=10$) yields 18.16% which is

Table 1: Performance comparison of different methods applied to LoRA on LLAMA2-7B weights across six common sense reasoning tasks with a validation set split from the training dataset. The best and the second best performances are specified in **boldface** and via underline respectively.

Metric	Method	Datasets					
		WG-S	ARC-C	ARC-E	WG-M	OBQA	BoolQ
ACC \uparrow	MAP	69.37 \pm 1.04	67.67 \pm 1.18	85.20 \pm 0.63	74.57 \pm 0.73	81.60 \pm 0.40	87.68 \pm 0.02
	MCD	69.06 \pm 1.40	66.66 \pm 2.30	85.49 \pm 0.74	75.89 \pm 0.48	81.46 \pm 0.92	87.67 \pm 0.08
	Deep Ensemble	68.98 \pm 0.97	68.57 \pm 2.11	86.24 \pm 1.26	77.39 \pm 1.08	82.20 \pm 0.91	88.07 \pm 0.17
	LA	68.18 \pm 1.04	64.17 \pm 0.97	85.30 \pm 0.97	74.15 \pm 0.40	77.53 \pm 0.80	86.45 \pm 0.35
	BLoB (M=0)	69.95 \pm 0.95	69.25 \pm 0.33	85.79 \pm 0.83	75.52 \pm 0.36	81.85 \pm 0.53	86.63 \pm 0.52
	BLoB (M=10)	66.55 \pm 0.61	66.66 \pm 2.25	84.56 \pm 0.20	73.38 \pm 0.29	81.44 \pm 0.53	86.63 \pm 0.50
	C-LoRA (M=0)	67.16 \pm 0.27	69.02 \pm 1.03	84.74 \pm 0.20	72.09 \pm 2.70	81.13 \pm 1.00	85.84 \pm 0.67
C-LoRA (M=10)	66.21 \pm 1.24	67.79 \pm 1.27	84.38 \pm 0.67	70.48 \pm 1.71	78.26 \pm 2.61	84.64 \pm 0.81	
ECE \downarrow	MAP	29.76 \pm 1.08	30.60 \pm 1.26	13.49 \pm 0.63	23.01 \pm 0.44	15.30 \pm 0.11	5.93 \pm 0.36
	MCD	28.49 \pm 1.60	29.60 \pm 2.77	12.69 \pm 0.60	20.73 \pm 0.38	14.34 \pm 1.11	5.13 \pm 0.25
	Deep Ensemble	28.72 \pm 1.46	27.75 \pm 1.86	11.87 \pm 0.16	18.67 \pm 0.29	13.98 \pm 1.12	5.24 \pm 0.27
	LA	11.41 \pm 0.17	30.54 \pm 0.70	45.85 \pm 2.08	10.80 \pm 0.38	35.65 \pm 1.14	18.22 \pm 0.41
	BLoB (M=0)	21.22 \pm 1.67	22.57 \pm 1.24	10.13 \pm 0.39	12.35 \pm 0.86	9.35 \pm 1.08	2.90 \pm 0.18
	BLoB (M=10)	11.23 \pm 1.45	<u>10.77</u> \pm 1.91	<u>4.29</u> \pm 1.08	<u>4.52</u> \pm 0.91	3.82 \pm 0.96	1.46 \pm 0.36
	C-LoRA (M=0)	<u>7.16</u> \pm 2.92	12.28 \pm 1.01	5.75 \pm 1.00	6.07 \pm 4.85	5.10 \pm 1.36	1.46 \pm 0.85
C-LoRA (M=10)	6.86 \pm 3.99	8.83 \pm 1.20	4.27 \pm 1.24	3.71 \pm 1.30	<u>4.00</u> \pm 0.84	<u>1.62</u> \pm 0.44	
NLL \downarrow	MAP	2.86 \pm 0.23	3.07 \pm 0.09	1.13 \pm 0.10	1.26 \pm 0.12	1.04 \pm 0.02	0.34 \pm 0.00
	MCD	2.50 \pm 0.12	2.81 \pm 0.25	1.13 \pm 0.04	1.16 \pm 0.03	1.01 \pm 0.07	<u>0.32</u> \pm 0.00
	Deep Ensemble	2.44 \pm 0.23	2.20 \pm 0.03	0.91 \pm 0.05	1.04 \pm 0.09	0.87 \pm 0.03	<u>0.32</u> \pm 0.00
	LA	0.62 \pm 0.00	1.17 \pm 0.01	0.97 \pm 0.05	<u>0.56</u> \pm 0.00	0.98 \pm 0.01	0.45 \pm 0.00
	BLoB (M=0)	0.90 \pm 0.07	1.34 \pm 0.05	0.63 \pm 0.02	0.61 \pm 0.03	0.59 \pm 0.02	0.31 \pm 0.00
	BLoB (M=10)	0.66 \pm 0.01	0.88 \pm 0.03	0.44 \pm 0.00	0.54 \pm 0.00	0.51 \pm 0.01	0.31 \pm 0.01
	C-LoRA (M=0)	0.64 \pm 0.03	<u>0.89</u> \pm 0.09	<u>0.46</u> \pm 0.01	0.58 \pm 0.03	<u>0.53</u> \pm 0.01	0.34 \pm 0.01
C-LoRA (M=10)	<u>0.63</u> \pm 0.02	0.88 \pm 0.00	0.48 \pm 0.02	0.57 \pm 0.03	0.59 \pm 0.05	0.35 \pm 0.02	

Table 2: Performance comparison of uncertainty quantification based on the ECE metric with temperature scaling using validation sets over six common-sense reasoning tasks.

Metric	Method	Datasets					
		WG-S	ARC-C	ARC-E	WG-M	OBQA	BoolQ
ECE \downarrow	BLoB (N=0)	21.22 \pm 1.67	22.57 \pm 1.24	10.13 \pm 0.39	12.35 \pm 0.86	9.35 \pm 1.08	2.90 \pm 0.18
	BLoB (M=0, tmp)	13.54 \pm 1.19	15.47 \pm 0.73	6.16 \pm 0.40	5.76 \pm 0.40	4.56 \pm 0.95	1.89 \pm 0.37
	BLoB (M=10)	11.23 \pm 1.45	10.77 \pm 1.91	4.29 \pm 1.08	4.52 \pm 0.91	3.82 \pm 0.96	1.46 \pm 0.36
	BLoB (M=10, tmp)	<u>5.10</u> \pm 1.47	6.87 \pm 1.91	5.38 \pm 1.08	<u>3.18</u> \pm 0.62	5.71 \pm 0.80	3.40 \pm 0.67
	C-LoRA (M=0)	<u>7.16</u> \pm 2.92	12.28 \pm 1.01	5.75 \pm 1.00	6.07 \pm 4.85	5.10 \pm 1.36	1.46 \pm 0.85
	C-LoRA (M=0, tmp)	4.00 \pm 1.37	<u>6.58</u> \pm 0.76	3.86 \pm 0.17	2.90 \pm 0.12	4.90 \pm 2.16	1.78 \pm 0.56
	C-LoRA (M=10)	6.86 \pm 3.99	8.83 \pm 1.20	<u>4.27</u> \pm 1.24	3.71 \pm 1.30	<u>4.00</u> \pm 0.84	<u>1.62</u> \pm 0.44
	C-LoRA (M=10, tmp)	5.18 \pm 1.54	6.30 \pm 0.87	4.35 \pm 1.35	3.87 \pm 1.77	6.27 \pm 1.01	2.67 \pm 0.29

only slightly worse than BLoB and significantly better than all other baselines. This indicates that C-LoRA remains well-calibrated even as the input distribution diverges from training. C-LoRA also excels in negative log-likelihood (NLL), achieving the lowest or second-lowest values across nearly all OOD datasets. On Chem and Phy, for example, C-LoRA (M=10) obtains NLL of 1.31 and 1.42 respectively, both lower than Deep Ensemble (1.45 and 1.58) and BLoB (1.35 and 1.46) and significantly better than all other baselines. Moreover, it is noteworthy that C-LoRA (M=0), which uses only the posterior mean, also maintains competitive performance. For example, on ARC-C and ARC-E, C-LoRA (M=0) achieves 10.08% and 6.42% ECE respectively, compared to BLoB (M=10)’s 9.77% and 5.74%. This suggests that C-LoRA’s contextual posterior mean already captures meaningful uncertainty, making it attractive for deployment in compute-constrained scenarios.

4.4 Ablation Study: Impact of Contextual Module

We also conduct the ablation study investigating the importance of the contextual module for overall performance. Since in C-LoRA we focus on contextualizing the distribution of matrix $\mathbf{E} \in \mathbb{R}^{r \times r}$, to examine the effect of the contextual module, we compare with the results of fine-tuning the model on

Table 3: Performance comparison on out-of-distribution datasets. The following results are evaluated using LLaMA2-7B fine-tuned on the OBQA dataset in Table 1.

Metric	Method	Datasets				
		<i>In-Dist.</i>	<i>Smaller Dist. Shift</i>		<i>Larger Dist. Shift</i>	
		OBQA	ARC-C	ARC-E	Chem	Phy
ACC \uparrow	MAP	81.60 \pm 0.40	67.67 \pm 1.52	73.88 \pm 0.27	41.00 \pm 3.60	33.00 \pm 5.29
	MCD	81.46 \pm 0.92	68.69 \pm 0.85	75.00 \pm 2.13	39.00 \pm 3.00	31.00 \pm 6.24
	Deep Ensemble	82.20 \pm 0.91	68.01 \pm 1.28	74.05 \pm 0.50	42.33 \pm 3.51	27.66 \pm 2.51
	BLoB (M=0)	81.85 \pm 0.53	69.48 \pm 0.78	76.93 \pm 1.33	45.33 \pm 1.15	26.66 \pm 4.61
	BLoB (M=10)	81.44 \pm 0.53	67.22 \pm 1.17	75.11 \pm 1.25	44.00 \pm 0.00	33.66 \pm 2.08
	C-LoRA (M=0)	81.13 \pm 1.00	66.66 \pm 0.78	75.99 \pm 1.63	40.00 \pm 1.73	28.00 \pm 1.73
	C-LoRA (M=10)	78.26 \pm 2.61	65.09 \pm 4.68	74.29 \pm 2.90	41.00 \pm 2.64	31.00 \pm 1.00
ECE \downarrow	MAP	15.30 \pm 0.11	25.54 \pm 1.25	20.09 \pm 0.53	29.73 \pm 0.30	36.22 \pm 3.60
	MCD	14.34 \pm 1.11	23.41 \pm 0.74	18.36 \pm 1.03	28.67 \pm 0.77	36.53 \pm 4.30
	Deep Ensemble	13.98 \pm 1.12	20.90 \pm 1.05	16.89 \pm 0.80	16.10 \pm 2.22	26.74 \pm 3.23
	BLoB (M=0)	9.35 \pm 1.08	15.76 \pm 1.42	11.70 \pm 0.62	14.12 \pm 4.05	27.35 \pm 4.01
	BLoB (M=10)	3.82 \pm 0.96	9.77 \pm 0.91	5.74 \pm 0.91	12.63 \pm 0.11	17.56 \pm 2.81
	C-LoRA (M=0)	5.10 \pm 1.36	10.08 \pm 3.30	6.42 \pm 2.48	15.42 \pm 2.99	24.42 \pm 6.02
	C-LoRA (M=10)	4.00 \pm 0.84	8.83 \pm 1.44	6.68 \pm 0.71	12.49 \pm 1.18	18.16 \pm 1.52
NLL \downarrow	MAP	1.04 \pm 0.02	1.66 \pm 0.12	1.37 \pm 0.04	1.81 \pm 0.03	1.86 \pm 0.04
	MCD	1.01 \pm 0.07	1.58 \pm 0.01	1.24 \pm 0.03	1.81 \pm 0.03	1.88 \pm 0.10
	Deep Ensemble	0.87 \pm 0.03	1.15 \pm 0.09	0.94 \pm 0.06	1.45 \pm 0.01	1.58 \pm 0.09
	BLoB (M=0)	0.59 \pm 0.02	0.95 \pm 0.05	0.72 \pm 0.01	1.41 \pm 0.02	1.57 \pm 0.03
	BLoB (M=10)	0.51 \pm 0.01	0.83 \pm 0.02	0.63 \pm 0.01	1.35 \pm 0.01	1.46 \pm 0.01
	C-LoRA (M=0)	0.53 \pm 0.01	0.85 \pm 0.04	0.64 \pm 0.04	1.43 \pm 0.01	1.54 \pm 0.09
	C-LoRA (M=10)	0.59 \pm 0.05	0.89 \pm 0.09	0.67 \pm 0.02	1.31 \pm 0.02	1.42 \pm 0.01

different tasks using lightweight factorization introduced in Section 3.1, with mean-field variational inference without the contextual module; we refer to this setting as **FE** in Tables 4 and 5.

Table 4 underscores the importance of the contextual module by comparing FE and C-LoRA across the six common-sense reasoning tasks under in-distribution scenario. C-LoRA offers significant improvements with respect to ECE across almost all tasks for inference-time sample with both M=0 and M=10, except for BoolQ where it achieves the second best performance. Also, C-LoRA gives the lowest NLL across all tasks.

Furthermore, we assess the effect of the contextual module on generalization. Table 5 provides the performance comparison of the corresponding models fine-tuned on OBQA in Table 4 under similar distribution shifts as in Table 3. C-LoRA outperforms FE across all datasets in both smaller and larger distribution shifts, with respect to ECE. In addition, C-LoRA offers the lowest NLL on all tasks in both distribution shifts. With respect to accuracy, in all tasks C-LoRA achieves a comparable performance, except for Chem where it has a subpar performance; however, this shortcoming is a result of the tradeoff between a generalized model with a proper uncertainty quantification, and an overconfident model with a poor uncertainty estimation. In summary, these results indicate the significance of our auxiliary contextual module, particularly on enhancing the uncertainty quantification and generalization while maintaining competitive predictive performance.

5 Related Works

LLMs have demonstrated remarkable successes across a wide range of applications, including code generation, scientific reasoning, and open-domain question answering; however, they are also notorious for *hallucination*—a phenomenon in which the model generates fluent but factually incorrect or unsupported content that is not grounded in the input or external knowledge. To mitigate hallucination, a variety of strategies have been proposed, including Reinforcement Learning from Human Feedback (RLHF) to align model outputs with human preferences [60, 61], and Retrieval-Augmented Generation (RAG) to ground responses in external knowledge [62, 63]. Additionally, probabilistic methods such as BNNs [19, 20] and conformal prediction [64, 65] have been demonstrated to be able to quantify uncertainty and flag unreliable outputs. Recent work also shows the effectiveness of prompt-level interventions [66, 67] by carefully crafting instructions and uncertainty-aware prompts to reduce hallucinated content without altering the model architecture.

Table 4: Impact of the contextual module on performance. The performance comparison is conducted across six common-sense reasoning tasks with a validation set split from the training dataset.

Metric	Method	Datasets					
		WG-S	ARC-C	ARC-E	WG-M	OBQA	BoolQ
ACC \uparrow	FE (M=0)	65.45 \pm 1.36	68.35 \pm 1.02	85.32 \pm 0.39	73.47 \pm 2.36	80.46 \pm 0.11	84.70 \pm 0.45
	FE (M=10)	65.06 \pm 1.33	68.20 \pm 2.40	85.08 \pm 0.36	72.43 \pm 1.28	80.93 \pm 0.50	84.65 \pm 0.52
	C-LoRA (M=0)	67.16 \pm 0.27	69.02 \pm 1.03	84.74 \pm 0.20	72.09 \pm 2.70	81.13 \pm 1.00	85.84 \pm 0.67
	C-LoRA (M=10)	66.21 \pm 1.24	67.79 \pm 1.27	84.38 \pm 0.67	70.48 \pm 1.71	78.26 \pm 2.61	84.64 \pm 0.81
ECE \downarrow	FE (M=0)	23.76 \pm 1.64	27.26 \pm 0.90	12.23 \pm 0.25	14.90 \pm 1.98	11.23 \pm 0.35	2.57 \pm 0.13
	FE (M=10)	18.12 \pm 1.52	19.60 \pm 2.42	9.54 \pm 0.47	12.21 \pm 1.87	8.42 \pm 0.50	1.34 \pm 0.22
	C-LoRA (M=0)	7.16 \pm 2.92	12.28 \pm 1.01	5.75 \pm 1.00	6.07 \pm 4.85	5.10 \pm 1.36	1.46 \pm 0.85
	C-LoRA (M=10)	6.86 \pm 3.99	8.83 \pm 1.20	4.27 \pm 1.24	3.71 \pm 1.30	4.00 \pm 0.84	1.62 \pm 0.44
NLL \downarrow	FE (M=0)	0.89 \pm 0.07	1.85 \pm 0.11	0.85 \pm 0.05	0.69 \pm 0.03	0.68 \pm 0.04	0.34 \pm 0.00
	FE (M=10)	0.78 \pm 0.04	1.35 \pm 0.12	0.65 \pm 0.02	0.63 \pm 0.02	0.60 \pm 0.03	0.34 \pm 0.00
	C-LoRA (M=0)	<u>0.64</u> \pm 0.03	<u>0.89</u> \pm 0.09	0.46 \pm 0.01	<u>0.58</u> \pm 0.03	0.53 \pm 0.01	0.34 \pm 0.01
	C-LoRA (M=10)	0.63 \pm 0.02	0.88 \pm 0.00	<u>0.48</u> \pm 0.02	0.57 \pm 0.03	<u>0.59</u> \pm 0.05	<u>0.35</u> \pm 0.02

Table 5: Impact of the contextual module on generalization. The performance comparison is conducted on out-of-distribution datasets using LLaMA2-7B fine-tuned on OBQA dataset in Table 4.

Metric	Method	Datasets				
		<i>In-Dist.</i>	<i>Smaller Dist. Shift</i>		<i>Larger Dist. Shift</i>	
		OBQA	ARC-C	ARC-E	Chem	Phy
ACC \uparrow	FE (M=0)	80.46 \pm 0.11	68.91 \pm 1.22	74.72 \pm 0.63	45.00 \pm 1.73	31.66 \pm 3.51
	FE (M=10)	80.93 \pm 0.50	66.65 \pm 1.09	74.76 \pm 0.70	46.00 \pm 1.73	32.33 \pm 1.52
	C-LoRA (M=0)	81.13 \pm 1.00	66.66 \pm 0.78	75.99 \pm 1.63	40.00 \pm 1.73	28.00 \pm 1.73
	C-LoRA (M=10)	78.26 \pm 2.61	65.09 \pm 4.68	74.29 \pm 2.90	41.00 \pm 2.64	31.00 \pm 1.00
ECE \downarrow	FE (M=0)	11.23 \pm 0.35	18.44 \pm 1.51	14.65 \pm 0.49	20.02 \pm 2.26	31.75 \pm 3.20
	FE (M=10)	8.42 \pm 0.50	15.78 \pm 1.11	11.69 \pm 0.68	17.61 \pm 1.25	26.02 \pm 1.32
	C-LoRA (M=0)	5.10 \pm 1.36	<u>10.08</u> \pm 3.30	6.42 \pm 2.48	<u>15.42</u> \pm 2.99	<u>24.42</u> \pm 6.02
	C-LoRA (M=10)	4.00 \pm 0.84	8.83 \pm 1.44	<u>6.68</u> \pm 0.71	12.49 \pm 1.18	18.16 \pm 1.52
NLL \downarrow	FE (M=0)	0.68 \pm 0.04	1.03 \pm 0.01	0.87 \pm 0.01	1.53 \pm 0.05	1.77 \pm 0.03
	FE (M=10)	0.60 \pm 0.03	0.95 \pm 0.02	0.78 \pm 0.01	1.46 \pm 0.03	1.67 \pm 0.02
	C-LoRA (M=0)	0.53 \pm 0.01	0.85 \pm 0.04	0.64 \pm 0.04	<u>1.43</u> \pm 0.01	<u>1.54</u> \pm 0.09
	C-LoRA (M=10)	0.59 \pm 0.05	<u>0.89</u> \pm 0.09	<u>0.67</u> \pm 0.02	1.31 \pm 0.02	1.42 \pm 0.01

Our work connects to previous efforts in BNNs by introducing a Bayesian formulation over the LoRA layers; however, we extend this line of work by using a data-dependent lightweight low-rank factorization, where the intermediate matrix \mathbf{E} is modeled as random variables, enabling flexible and context-aware uncertainty estimation to mitigate overconfidence and hallucination in LLMs.

6 Conclusion

In this work, we introduced C-LoRA, a novel uncertainty-aware parameter-efficient approach for fine-tuning LLMs in an end-to-end Bayesian framework. C-LoRA facilitates modeling the aleatoric uncertainty (data uncertainty) via an efficient and scalable contextual module, without compromising the potential for estimating the model uncertainty. Through extensive empirical studies, we demonstrate the superior performance of our method in achieving outstanding accuracy and strong uncertainty quantification capabilities, with consistent generalization across diverse data distributions. Our method underscores the significance of modeling the aleatoric uncertainty in low-data regimes that can lead to substantial gains in generalization and trustworthiness of LLMs.

7 Limitations

Evaluating uncertainty in language models remains an open challenge due to the lack of standardized benchmarks with ground-truth uncertainty labels. While our evaluation—based on held-out test sets and established metrics like ECE and NLL—provides meaningful insight into model calibration and predictive confidence, these metrics offer only an indirect view of uncertainty quality. Developing task-specific benchmarks or human-in-the-loop protocols for evaluating uncertainty in NLP remains an important direction for future work.

References

- [1] Ola Shorinwa, Zhiting Mei, Justin Lidard, Allen Z. Ren, and Anirudha Majumdar. A survey on uncertainty quantification of large language models: Taxonomy, open research challenges, and future directions, 2024.
- [2] Shervin Minaee, Tomas Mikolov, Narjes Nikzad, Meysam Chenaghlu, Richard Socher, Xavier Amatriain, and Jianfeng Gao. Large language models: A survey, 2024.
- [3] Alec Radford, Jeffrey Wu, Rewon Child, David Luan, Dario Amodei, and Ilya Sutskever. Language models are unsupervised multitask learners. *OpenAI*, 2019. Accessed: 2024-11-15.
- [4] Tom B. Brown, Benjamin Mann, Nick Ryder, et al. Language models are few-shot learners, 2020.
- [5] OpenAI et al. Gpt-4 technical report, 2024.
- [6] Hugo Touvron et al. Llama 2: Open foundation and fine-tuned chat models, 2023.
- [7] Aaron Grattafiori et al. The llama 3 herd of models, 2024.
- [8] Haotian Cui, Chloe Wang, Hassaan Maan, Kuan Pang, Fengning Luo, Nan Duan, and Bo Wang. scgpt: toward building a foundation model for single-cell multi-omics using generative ai. *Nature Methods*, 21(8):1470–1480, Aug 2024.
- [9] Renqian Luo, Liai Sun, Yingce Xia, Tao Qin, Sheng Zhang, Hoifung Poon, and Tie-Yan Liu. Biogpt: generative pre-trained transformer for biomedical text generation and mining. *Briefings in Bioinformatics*, 23(6), September 2022.
- [10] Karan Singhal, Shekoofeh Azizi, Tao Tu, et al. Publisher correction: Large language models encode clinical knowledge. *Nature*, 620(7973):E19, 2023.
- [11] Xi Yang, Aokun Chen, Nima PourNejatian, et al. Gatortron: A large clinical language model to unlock patient information from unstructured electronic health records, 2022.
- [12] Sanket Jantre, Tianle Wang, Gilchan Park, Kriti Chopra, Nicholas Jeon, Xiaoning Qian, Nathan M Urban, and Byung-Jun Yoon. Uncertainty-aware adaptation of large language models for protein-protein interaction analysis. *arXiv preprint arXiv:2502.06173*, 2025.
- [13] Andres M Bran, Sam Cox, Oliver Schilter, Carlo Baldassari, Andrew D White, and Philippe Schwaller. Chemcrow: Augmenting large-language models with chemistry tools, 2023.
- [14] Ross Taylor, Marcin Kardas, Guillem Cucurull, Thomas Scialom, Anthony Hartshorn, Elvis Saravia, Andrew Poulton, Viktor Kerkez, and Robert Stojnic. Galactica: A large language model for science, 2022.
- [15] Hongyang Yang, Xiao-Yang Liu, and Christina Dan Wang. Fingpt: Open-source financial large language models, 2023.
- [16] Shijie Wu, Ozan Irsoy, Steven Lu, Vadim Dabravolski, Mark Dredze, Sebastian Gehrmann, Prabhanjan Kambadur, David Rosenberg, and Gideon Mann. Bloomberggpt: A large language model for finance, 2023.
- [17] David Thulke, Yingbo Gao, Petrus Pelsler, et al. Climategpt: Towards ai synthesizing interdisciplinary research on climate change, 2024.
- [18] Mark Chen, Jerry Tworek, Heewoo Jun, et al. Evaluating large language models trained on code, 2021.
- [19] Adam X. Yang, Maxime Robeyns, Xi Wang, and Laurence Aitchison. Bayesian low-rank adaptation for large language models, 2024.
- [20] Yibin Wang, Haizhou Shi, Ligong Han, Dimitris Metaxas, and Hao Wang. Blob: Bayesian low-rank adaptation by backpropagation for large language models, 2024.
- [21] Edward J. Hu, Yelong Shen, Phillip Wallis, Zeyuan Allen-Zhu, Yuanzhi Li, Shean Wang, Lu Wang, and Weizhu Chen. Lora: Low-rank adaptation of large language models, 2021.
- [22] Vladislav Lialin, Vijeta Deshpande, Xiaowei Yao, and Anna Rumshisky. Scaling down to scale up: A guide to parameter-efficient fine-tuning, 2024.
- [23] Yaqing Wang, Subhabrata Mukherjee, Xiaodong Liu, Jing Gao, Ahmed Hassan Awadallah, and Jianfeng Gao. List: Lite prompted self-training makes parameter-efficient few-shot learners, 2022.

- [24] Moxin Li, Wenjie Wang, Fuli Feng, Fengbin Zhu, Qifan Wang, and Tat-Seng Chua. Think twice before trusting: Self-detection for large language models through comprehensive answer reflection, 2024.
- [25] Miao Xiong, Zhiyuan Hu, Xinyang Lu, Yifei Li, Jie Fu, Junxian He, and Bryan Hooi. Can llms express their uncertainty? an empirical evaluation of confidence elicitation in llms, 2024.
- [26] Jixuan Leng, Chengsong Huang, Banghua Zhu, and Jiaxin Huang. Taming overconfidence in llms: Reward calibration in rlhf, 2024.
- [27] Guande He, Jianfei Chen, and Jun Zhu. Preserving pre-trained features helps calibrate fine-tuned language models, 2023.
- [28] Cristian Meo, Ksenia Sycheva, Anirudh Goyal, and Justin Dauwels. Bayesian-lora: Lora based parameter efficient fine-tuning using optimal quantization levels and rank values through differentiable bayesian gates, 2024.
- [29] Yarin Gal and Zoubin Ghahramani. Dropout as a bayesian approximation: Representing model uncertainty in deep learning. In *International Conference on Machine Learning*, 2016.
- [30] Qingping Zhou, Tengchao Yu, Xiaoqun Zhang, and Jinglai Li. Bayesian inference and uncertainty quantification for image reconstruction with poisson data, 2019.
- [31] Mohammad Hossein Shaker and Eyke Hüllermeier. Ensemble-based uncertainty quantification: Bayesian versus credal inference, 2021.
- [32] Ziyu Wang and Chris Holmes. On uncertainty quantification for near-bayes optimal algorithms, 2024.
- [33] Ethan Goan and Clinton Fookes. *Bayesian Neural Networks: An Introduction and Survey*, page 45–87. Springer International Publishing, 2020.
- [34] Erik Daxberger, Agustinus Kristiadi, Alexander Immer, Runa Eschenhagen, Matthias Bauer, and Philipp Hennig. Laplace redux – effortless bayesian deep learning, 2022.
- [35] Shujian Zhang, Xinjie Fan, Bo Chen, and Mingyuan Zhou. Bayesian attention belief networks, 2021.
- [36] Ruqi Zhang, Chunyuan Li, Jianyi Zhang, Changyou Chen, and Andrew Gordon Wilson. Cyclical stochastic gradient mcmc for bayesian deep learning, 2020.
- [37] Agustinus Kristiadi, Matthias Hein, and Philipp Hennig. Being bayesian, even just a bit, fixes overconfidence in relu networks, 2020.
- [38] Alex Kendall and Yarin Gal. What uncertainties do we need in bayesian deep learning for computer vision?, 2017.
- [39] Xinjie Fan, Shujian Zhang, Korawat Tanwisuth, Xiaoning Qian, and Mingyuan Zhou. Contextual dropout: An efficient sample-dependent dropout module, 2021.
- [40] Sanket Jantre, Shrijita Bhattacharya, Nathan M Urban, Byung-Jun Yoon, Tapabrata Maiti, Prasanna Balaprakash, and Sandeep Madireddy. Sequential Bayesian neural subnetwork ensembles. *arXiv:2206.00794*, 2022.
- [41] Sanket Jantre, Nathan M. Urban, Xiaoning Qian, and Byung-Jun Yoon. Learning active subspaces for effective and scalable uncertainty quantification in deep neural networks. In *IEEE International Conference on Acoustics, Speech and Signal Processing (ICASSP)*, 2024.
- [42] David M. Blei, Alp Kucukelbir, and Jon D. McAuliffe and. Variational inference: A review for statisticians. *Journal of the American Statistical Association*, 112(518):859–877, 2017.
- [43] Matt Hoffman, David M. Blei, Chong Wang, and John Paisley. Stochastic variational inference, 2013.
- [44] Ning Ding, Yujia Qin, Guang Yang, et al. Parameter-efficient fine-tuning of large-scale pre-trained language models. *Nature Machine Intelligence*, 5(3):220–235, Mar 2023.
- [45] Haokun Liu, Derek Tam, Mohammed Muqeeth, Jay Mohta, Tenghao Huang, Mohit Bansal, and Colin Raffel. Few-shot parameter-efficient fine-tuning is better and cheaper than in-context learning, 2022.
- [46] Zhengxiang Shi and Aldo Lipani. Dept: Decomposed prompt tuning for parameter-efficient fine-tuning, 2024.

- [47] Zeyu Han, Chao Gao, Jinyang Liu, Jeff Zhang, and Sai Qian Zhang. Parameter-efficient fine-tuning for large models: A comprehensive survey, 2024.
- [48] Ali Edalati, Marzieh Tahaei, Ivan Kobyzev, Vahid Partovi Nia, James J. Clark, and Mehdi Rezagholizadeh. Krona: Parameter efficient tuning with kronecker adapter, 2022.
- [49] Oleksandr Balabanov and Hampus Linander. Uncertainty quantification in fine-tuned llms using lora ensembles, 2024.
- [50] Emre Onal, Klemens Flöge, Emma Caldwell, Arsen Sheverdin, and Vincent Fortuin. Gaussian stochastic weight averaging for bayesian low-rank adaptation of large language models, 2024.
- [51] Xi Wang, Laurence Aitchison, and Maja Rudolph. Lora ensembles for large language model fine-tuning, 2023.
- [52] Durk P Kingma, Tim Salimans, and Max Welling. Variational dropout and the local reparameterization trick. *Advances in neural information processing systems*, 28, 2015.
- [53] Balaji Lakshminarayanan, Alexander Pritzel, and Charles Blundell. Simple and scalable predictive uncertainty estimation using deep ensembles, 2017.
- [54] Sourab Mangrulkar, Sylvain Gugger, Lysandre Debut, Younes Belkada, Sayak Paul, and Benjamin Bossan. Pefit: State-of-the-art parameter-efficient fine-tuning methods. <https://github.com/huggingface/peft>, 2022.
- [55] Keisuke Sakaguchi, Ronan Le Bras, Chandra Bhagavatula, and Yejin Choi. Winogrande: An adversarial winograd schema challenge at scale, 2019.
- [56] Peter Clark, Isaac Cowhey, Oren Etzioni, Tushar Khot, Ashish Sabharwal, Carissa Schoenick, and Oyvind Tafjord. Think you have solved question answering? try arc, the ai2 reasoning challenge, 2018.
- [57] Todor Mihaylov, Peter Clark, Tushar Khot, and Ashish Sabharwal. Can a suit of armor conduct electricity? a new dataset for open book question answering, 2018.
- [58] Christopher Clark, Kenton Lee, Ming-Wei Chang, Tom Kwiatkowski, Michael Collins, and Kristina Toutanova. Boolq: Exploring the surprising difficulty of natural yes/no questions, 2019.
- [59] Chuan Guo, Geoff Pleiss, Yu Sun, and Kilian Q. Weinberger. On calibration of modern neural networks, 2017.
- [60] Yuxin Liang, Zhuoyang Song, Hao Wang, and Jiaying Zhang. Learning to trust your feelings: Leveraging self-awareness in llms for hallucination mitigation. *arXiv preprint arXiv:2401.15449*, 2024.
- [61] Xueru Wen, Xinyu Lu, Xinyan Guan, Yaojie Lu, Hongyu Lin, Ben He, Xianpei Han, and Le Sun. On-policy fine-grained knowledge feedback for hallucination mitigation. *arXiv preprint arXiv:2406.12221*, 2024.
- [62] Patrick Lewis, Ethan Perez, Aleksandra Piktus, Fabio Petroni, Vladimir Karpukhin, Naman Goyal, Heinrich Küttler, Mike Lewis, Wen-tau Yih, Tim Rocktäschel, et al. Retrieval-augmented generation for knowledge-intensive nlp tasks. *Advances in neural information processing systems*, 33:9459–9474, 2020.
- [63] Yunfan Gao, Yun Xiong, Xinyu Gao, Kangxiang Jia, Jinliu Pan, Yuxi Bi, Yixin Dai, Jiawei Sun, Haofen Wang, and Haofen Wang. Retrieval-augmented generation for large language models: A survey. *arXiv preprint arXiv:2312.10997*, 2:1, 2023.
- [64] Bhawesh Kumar, Charlie Lu, Gauri Gupta, Anil Palepu, David Bellamy, Ramesh Raskar, and Andrew Beam. Conformal prediction with large language models for multi-choice question answering. *arXiv preprint arXiv:2305.18404*, 2023.
- [65] Victor Quach, Adam Fisch, Tal Schuster, Adam Yala, Jae Ho Sohn, Tommi S Jaakkola, and Regina Barzilay. Conformal language modeling. *arXiv preprint arXiv:2306.10193*, 2023.
- [66] Mingjian Jiang, Yangjun Ruan, Sicong Huang, Saifei Liao, Silviu Pitis, Roger Baker Grosse, and Jimmy Ba. Calibrating language models via augmented prompt ensembles. In *Workshop on Challenges in Deployable Generative AI at International Conference on Machine Learning (ICML)*, 2023.
- [67] Yasin Abbasi Yadkori, Ilja Kuzborskij, András György, and Csaba Szepesvári. To believe or not to believe your llm. *arXiv preprint arXiv:2406.02543*, 2024.
- [68] Kevin P. Murphy. *Probabilistic Machine Learning: Advanced Topics*. MIT Press, 2023.
- [69] Yeming Wen, Paul Vicol, Jimmy Ba, Dustin Tran, and Roger Grosse. Flipout: Efficient pseudo-independent weight perturbations on mini-batches. In *International Conference on Learning Representations*, 2018.

A Dataset Details

A brief summary of the prompt templates used for fine-tuning LLaMA2 on common-sense reasoning tasks is provided in Table 6. More details on the size of training datasets after applying an 80% train-validation split, and the number of labels are gathered in Table 7.

Table 6: Prompt templates for fine-tuning on common-sense reasoning tasks

task	prompt
Winogrande (WG-S/WG-M)	Select one of the choices that answers the following question: {question} Choices: A. {option1}. B. {option2}. Answer:
ARC (ARC-C/ARC-E), Openbook QA (OBQA), MMLU	Select one of the choices that answers the following question: {question} Choices: A. {choice1}. B. {choice2}, C. {choice3}. D. {choice4}. Answer:
BoolQ	Answer the question with only True or False: {question} Context: {passage}

Table 7: Size of the training dataset after train-validation split and number of labels in each dataset

	WG-S	ARC-C	ARC-E	WG-M	OBQA	BoolQ
Training dataset size	512	892	1.8K	2.05k	3.97k	1.99k
Number of labels	2	5	5	2	4	2

B Temperature Scaling

Temperature scaling is a commonly adopted method to convert the predicted probabilities to more calibrated values [59, 68]. To do so, it employs a positive constant scaler, T , called the temperature parameter, to *soften* the softmax values making the distribution less peaky. That is, given the logit vector \mathbf{z} , the new confidence can be expressed as,

$$\mathbf{q} = \sigma(\mathbf{z}/T), \tag{9}$$

where σ is the softmax operator. It has been empirically shown in [59] that such temperature scaling leads to lower Expected Calibration Error (ECE) on classification tasks. Here, T can be estimated via optimizing the Negative Log-Likelihood (NLL) on the validation set. Since T does not change the maximum of the softmax function, the prediction is unaffected; therefore, it does not change the model’s accuracy while enhancing model’s calibration.

C Uncertainty Estimation Metrics

Uncertainty quantification is commonly assessed by NLL and ECE in the literature. The summation of the negative expected log probability of predicting the correct label is calculated for NLL. That is, for the model P_θ , and a dataset of size N , NLL is computed as,

$$\text{NLL} = \frac{1}{N} \sum_{i=1}^N -\log P_\theta(y_i), \tag{10}$$

where y_i denotes the correct label. This metric promotes the model to assign a higher probability to the correct predictions. For an overconfident model in an incorrect prediction, the probability of correct answer decreases, which leads to an increase in NLL. ECE on the other hand, estimates how well a model is calibrated by assessing how close the model’s confidence is to its accuracy. Specifically, by binning the predictions according to the confidence levels, this metric is calculated by the weighted average of the absolute difference in each bin, that is,

$$\text{ECE} = \sum_{m=1}^M \frac{|B_m|}{N} |\text{acc}(B_m) - \text{conf}(B_m)|, \tag{11}$$

where $\text{acc}(B_m)$ and $\text{conf}(B_m)$ indicate the average accuracy and confidence in each bin, B_m ,

$$\text{acc}(B_m) = \frac{1}{|B_m|} \sum_{i \in B_m} \mathbf{1}(\hat{y}_i = y_i), \quad \text{conf}(B_m) = \frac{1}{|B_m|} \sum_{i \in B_m} P(\hat{y}_i), \quad (12)$$

in which $|B_m|$ denotes the number of examples in bin m .

D Hyperparameters

Table 8 summarizes the hyperparameters for LoRA fine-tuning of LLaMA2-7B, selected based on prior work [19–21] and default values provided in PEFT library [54]. Following [20], we optimize the KL term with SGD and a linear learning-rate scheduler.

Table 8: Hyperparameters of LoRA fine-tuning of LLaMA2-7B

Hyper-parameter	Value
Optimizer	AdamW
LR Scheduler	Linear
Learning Rate	$1e-4$
Batch Size	4
Max Sequence Length	300
LoRA α	16
LoRA r	8

E On the Importance of Flexibility

To study the impact of complexity we examine the performance of FE with the case where the matrix \mathbf{E} is a diagonal matrix with r random variables. We refer to this as **DE**.

Table 9 summarizes the performance of DE and FE with $M=0$ and $M=10$ under in-distribution scenario for the six common-sense reasoning tasks. These models are ordered from top to bottom for each metric, such that each successive model is more flexible than the previous one. From Table 9, it is clear that as the flexibility increases, the performance generally improves. Specifically, in almost all tasks, FE provides a better uncertainty quantification with respect to DE, with a lower ECE and NLL. Although FE does not always deliver the highest accuracy, it shows a comparable performance across all tasks. Particularly, it provides the best accuracy in ARC-C under both deterministic ($M=0$) and stochastic ($M=10$) settings. It can be concluded from Table 9 that a more flexible model yields more reliable uncertainty quantification, with no significant loss in predictive accuracy.

To assess the effect of model complexity on generalization, we further compared DE and FE under out-of-distribution scenario, using the models fine-tuned on OBQA from Table 9. As Table 10 indicates, FE consistently delivers superior uncertainty quantification over all tasks under both smaller and larger distribution shifts. It also delivers the best accuracy in almost all tasks.

These findings from Tables 9 and 10 confirm that richer stochastic structures enhance both generalization and uncertainty estimation, motivating our focus on contextualizing the full matrix \mathbf{E} .

F Checkpoint Metric

Given our goal of achieving a well-calibrated model while maintaining competitive accuracy relative to the states of the art (SOTAs), we devise a metric that incorporates both accuracy (ACC) and expected calibration error (ECE). Specifically, we define:

$$\mathcal{C} = (1 - \text{ACC}_{\text{val}}) \cdot \text{ECE}_{\text{val}},$$

with ACC_{val} and ECE_{val} representing the validation accuracy and expected calibration error, respectively. During training, the model is evaluated using this criterion every 100 steps. We summarize the training algorithm of C-LoRA in Algorithm 1.

Table 9: Impact of different levels of flexibility on performance. Performance comparison is conducted across six common-sense reasoning tasks with a validation set split from the training dataset. The best and the second best performances are specified in **boldface** and via underline respectively.

Metric	Method	Datasets					
		WG-S	ARC-C	ARC-E	WG-M	OBQA	BoolQ
ACC \uparrow	DE (M=0)	65.98 \pm 2.46	66.77 \pm 1.28	85.61 \pm 0.36	75.19 \pm 0.05	81.80 \pm 1.05	87.47 \pm 0.03
	DE (M=10)	66.09 \pm 1.50	66.88 \pm 1.47	85.71 \pm 0.64	75.19 \pm 0.16	82.06 \pm 0.41	87.44 \pm 0.07
	FE (M=0)	65.45 \pm 1.36	68.35 \pm 1.02	85.32 \pm 0.39	73.47 \pm 2.36	80.46 \pm 0.11	84.70 \pm 0.45
	FE (M=10)	65.06 \pm 1.33	68.20 \pm 2.40	85.08 \pm 0.36	72.43 \pm 1.28	80.93 \pm 0.50	84.65 \pm 0.52
ECE \downarrow	DE (M=0)	30.99 \pm 1.39	29.63 \pm 1.58	13.17 \pm 0.30	21.91 \pm 0.49	14.19 \pm 0.37	4.67 \pm 0.17
	DE (M=10)	27.00 \pm 0.62	<u>26.26</u> \pm 1.17	11.79 \pm 0.16	20.21 \pm 0.09	13.24 \pm 0.34	4.41 \pm 0.02
	FE (M=0)	<u>23.76</u> \pm 1.64	27.26 \pm 0.90	12.23 \pm 0.25	<u>14.90</u> \pm 1.98	<u>11.23</u> \pm 0.35	<u>2.57</u> \pm 0.13
	FE (M=10)	18.12 \pm 1.52	19.60 \pm 2.42	9.54 \pm 0.47	12.21 \pm 1.87	8.42 \pm 0.50	1.34 \pm 0.22
NLL \downarrow	DE (M=0)	2.14 \pm 0.00	2.83 \pm 0.26	1.17 \pm 0.08	1.18 \pm 0.06	0.91 \pm 0.02	0.32 \pm 0.00
	DE (M=10)	1.58 \pm 0.05	2.21 \pm 0.06	1.05 \pm 0.07	1.05 \pm 0.05	0.85 \pm 0.02	0.32 \pm 0.00
	FE (M=0)	0.89 \pm 0.07	<u>1.85</u> \pm 0.11	0.85 \pm 0.05	0.69 \pm 0.03	0.68 \pm 0.04	0.34 \pm 0.00
	FE (M=10)	0.78 \pm 0.04	1.35 \pm 0.12	0.65 \pm 0.02	0.63 \pm 0.02	0.60 \pm 0.03	0.34 \pm 0.00

Table 10: Impact of different levels of complexity on generalization. Performance comparison is conducted on out-of-distribution datasets. The following results are evaluated using LLaMA2-7B fine-tuned on the OBQA dataset. The best and the second best performances are specified in **boldface** and via *underline* respectively.

Metric	Method	Datasets				
		<i>In-Dist.</i>	<i>Smaller Dist. Shift</i>		<i>Larger Dist. Shift</i>	
		OBQA	ARC-C	ARC-E	Chem	Phy
ACC \uparrow	DE (M=0)	81.80 \pm 1.05	68.46 \pm 1.92	74.75 \pm 0.79	44.33 \pm 2.08	31.00 \pm 4.35
	DE (M=10)	82.06 \pm 0.41	67.90 \pm 0.67	74.80 \pm 1.07	43.33 \pm 0.57	30.66 \pm 4.51
	FE (M=0)	80.46 \pm 0.11	68.91 \pm 1.22	74.72 \pm 0.63	45.00 \pm 1.73	31.66 \pm 3.51
	FE (M=10)	80.93 \pm 0.50	66.65 \pm 1.09	74.76 \pm 0.70	46.00 \pm 1.73	32.33 \pm 1.52
ECE \downarrow	DE (M=0)	14.19 \pm 0.37	23.51 \pm 2.07	17.74 \pm 0.64	23.37 \pm 3.97	34.33 \pm 2.34
	DE (M=10)	13.24 \pm 0.34	22.31 \pm 0.53	16.81 \pm 1.17	21.90 \pm 1.90	35.14 \pm 5.68
	FE (M=0)	11.23 \pm 0.35	<u>18.44</u> \pm 1.51	<u>14.65</u> \pm 0.49	<u>20.02</u> \pm 2.26	<u>31.75</u> \pm 3.20
	FE (M=10)	8.42 \pm 0.50	15.78 \pm 1.11	11.69 \pm 0.68	17.61 \pm 1.25	26.02 \pm 1.32
NLL \downarrow	DE (M=0)	0.91 \pm 0.02	1.35 \pm 0.08	1.08 \pm 0.03	1.64 \pm 0.06	1.86 \pm 0.05
	DE (M=10)	0.85 \pm 0.02	1.28 \pm 0.05	1.04 \pm 0.02	1.62 \pm 0.06	1.82 \pm 0.05
	FE (M=0)	0.68 \pm 0.04	<u>1.03</u> \pm 0.01	<u>0.87</u> \pm 0.01	<u>1.53</u> \pm 0.05	<u>1.77</u> \pm 0.03
	FE (M=10)	0.60 \pm 0.03	0.95 \pm 0.02	0.78 \pm 0.01	1.46 \pm 0.03	1.67 \pm 0.02

G Flipout

To speed up the sampling, we apply the Flipout technique—originally introduced in [69] and also adopted by [51]—in C-LoRA to the low-rank matrix \mathbf{E} . In particular, having two randomly sampled flipping vectors $s = \{-1, +1\}^r$ and $t = \{-1, +1\}^r$, and considering \mathbf{b}_i to be the i -th input in a mini-batch, the output after flipout is:

$$\mathbf{o}_i = \mathbf{W}\mathbf{b}_i = \mathbf{W}_0\mathbf{b}_i + \mathbf{B}\mathbf{E}\mathbf{A}\mathbf{b}_i = \mathbf{W}_0\mathbf{b}_i + \mathbf{B}(\boldsymbol{\mu}_{\mathbf{E}} + (\mathcal{E} \circ \boldsymbol{\Omega}_{\mathbf{E}}) \circ (t_i s_i^\top))\mathbf{A}\mathbf{b}_i, \quad \mathcal{E} \sim \mathcal{N}(\mathbf{0}, \mathbf{I})$$

H Discussion on Results of Laplace Approximation

For experiments involving fine-tuning via Laplace approximation (LA), we used the publicly released code provided by the authors of [19]. However, the results that we attempted to reproduce—reported in Table 1 in our main paper—are substantially worse than those reported in the original paper [19]. This discrepancy is especially pronounced for the OBQA and BoolQ datasets. Our findings are

Algorithm 1 Contextual Low-rank Adaptation (C-LoRA)

Require: Dataset split: $\mathcal{D}_{\text{train}}, \mathcal{D}_{\text{validation}}, \mathcal{D}_{\text{test}}$
Require: contextual module h_φ , deterministic parameters θ , number of iterations T , evaluation frequency f_{eval} , learning rate η , checkpoint metric b

- 1: $b \leftarrow \infty$
- 2: **for** $t \leftarrow 0$ to T **do**
- 3: $\mathbf{x}, y \sim \mathcal{D}_{\text{train}}$
- 4: $\mathbf{x}^0 \leftarrow \mathbf{x}$
- 5: **for** $l \leftarrow 1$ to L **do**
- 6: $\boldsymbol{\mu}_{\mathbf{E}}^l, \boldsymbol{\Omega}_{\mathbf{E}}^l \leftarrow h_\varphi^l(\mathbf{x}^{l-1})$
- 7: $\mathcal{E}^l \sim \mathcal{N}(\mathbf{0}, \mathbf{I})$
- 8: $\mathbf{E}_{\mathbf{x}}^l \leftarrow \text{Flipout}(\mathcal{E}^l)$
- 9: **end for**
- 10: $\boldsymbol{\theta} \leftarrow \boldsymbol{\theta} - \eta \nabla_{\boldsymbol{\theta}} \mathcal{L}(\mathbf{x}, y)$ ▷ Eq. 7
- 11: $\varphi \leftarrow \varphi - \eta \nabla_{\varphi} \mathcal{L}(\mathbf{x}, y)$ ▷ Eq. 8
- 12: **if** $t \bmod f_{\text{eval}} = 0$ **then**
- 13: Compute validation accuracy and ECE
- 14: $\tilde{b} \leftarrow (1 - \text{ACC}_{\text{val}}) \cdot \text{ECE}_{\text{val}}$
- 15: **if** $\tilde{b} < b$ **then**
- 16: $b \leftarrow \tilde{b}$
- 17: Save $\boldsymbol{\theta}, \varphi$ ▷ Checkpoint best model
- 18: Record performance on $\mathcal{D}_{\text{test}}$
- 19: **end if**
- 20: **end if**
- 21: **end for**

consistent with those reported by the authors of BLoB [20], which suggests that the degradation in performance may stem from sub-optimal MAP solutions that negatively impact the quality of the Laplace approximation-based LoRA fine-tuning.

Additionally, in our experiments, we observed that LA is notably memory-intensive, requiring hardware with higher memory capacity than BLoB and our C-LoRA implementations. This might make the practical applicability of LA more challenging considering the scalability compared to other competing methods.

I Broader Impacts

Our uncertainty-aware fine-tuning framework integrating uncertainty quantification in LLMs could enhance the safety, reliability, and trustworthiness of AI systems deployed in high-stakes settings such as medical diagnosis, atmospheric modeling, and autonomous navigation, where unrecognized model errors can have major consequences. Moreover, as our approach explicitly models aleatoric or data uncertainty, it is particularly well-suited for low-resource tasks and rare-event prediction, providing access to robust LLM-based AI tools in fields ranging from global health to societal governance and policy-making.

We anticipate minimal additional computational overhead compared to standard fine-tuning, and because our framework is compatible with existing Bayesian extensions for epistemic uncertainty, it offers a clear path toward unified uncertainty quantification without introducing undue complexity. We do not foresee any negative societal impacts beyond those already inherent to large-scale model deployment, and we believe that equipping models with calibrated confidence measures is an essential step toward more ethical, accountable, and human-centered AI.

J Additional Information

In our contextual module, we set C , the number of hidden units, to 64 in order to ensure sufficient expressiveness for learning meaningful features. Also, to have a robust performance, the variance output, $\boldsymbol{\Omega}_{\mathbf{E}}$, uses a sigmoid activation function; however, we do not use any activation function for

the mean μ_E . All the experiments for almost all methods were conducted using 1 NVIDIA A100 GPU with 40 GB memory except for BLoB, for which we used 2 NVIDIA A100 with 40 GB memory. Also for LA we used NVIDIA L40S GPU with 48 GB memory due to its memory demands.